

# Design of Gamma Ray Detectors and Associated Readout Electronics for a Time Reversal Experiment

Tine Valencic, Caltech      Mentor: John Behr, TRIUMF  
Co-Mentor: Petr Vogel, Caltech

September 30, 2018

## Abstract

The TRIUMF Neutral Atom Trap (TRINAT) experiment looks at beta decay in radioactive isotopes of alkali metals ( $^{92}\text{Rb}$  and  $^{38m}\text{K}$ ) and searches for time-reversal symmetry violations on MeV scales. Detection is accomplished by measuring the momenta of three products of the decay – the beta particle, the gamma ray, and the recoiling nucleus. Time reversal is simulated conceptually by flipping the momenta of the three decay products, then smoothly rotating the result to target specific detectors. Asymmetries are present if, when the momenta are flipped, the number of events in the gamma detector changes. Such an observable is not sensitive to spin so, if detected, would point toward new physics different from contributions to the neutron electric dipole moment. Various scintillating materials were tested for their energy resolution, light output, and timing properties while a readout circuit was designed. Two bismuth germanate (BGO) crystals with silicon photomultiplier (SiPM) readout were then tested, calibrated, and mounted symmetrically on the atom trap.

## Background

The excess of matter relative to antimatter points to an asymmetry in baryon generation in the early universe. Sakharov [1] showed that violation of charge-parity symmetry (equivalent to time reversal if CPT is conserved) may result in such an imbalance. The TRINAT experiment looks for a time-reversal violating (TRV) asymmetry in the radiative  $\beta$  decays of  $^{38m}\text{K}$  and  $^{92}\text{Rb}$ . This requires determining the momenta of three products of the decay: the recoiling nucleus, the beta particle, and the radiating gamma ray. Such TRV correlations have been searched for in studies of meson decay but never in the first generation of particles [2]. My work this summer focused on constructing and calibrating a pair of detectors to determine the energy spectrum of the gamma ray which is produced in a small fraction (roughly 3% [3]) of decays of  $^{92}\text{Rb}$ .

## Time reversal modeled by momentum flips

The idea of time reversal is simple mathematically: one switches the sign on time, or formally

$$t \mapsto -t$$

If we apply such a reversal to momentum, we see that

$$p = m \frac{d\mathbf{r}}{dt} \mapsto m \frac{d\mathbf{r}}{d(-t)} = -m \frac{d\mathbf{r}}{dt} = -p$$

Thus, momentum is a quantity which changes sign when the time reversal operator acts upon it. Now, consider the triple product of the three momenta (the recoiling nucleus, the beta particle, and the gamma ray) measured in the experiment:

$$p_{recoil} \cdot (p_{\beta} \times p_{\gamma})$$

When the time reversal operator  $t \mapsto -t$  is applied to this quantity, all three momenta acquire a negative sign, so

$$p_{recoil} \cdot (p_\beta \times p_\gamma) \xrightarrow{t \mapsto -t} -p_{recoil} \cdot (p_\beta \times p_\gamma)$$

Therefore, changing the sign of this triple product results in effects similar to time reversal. If the weak force (which drives beta decay) is symmetric in time, the triple product should have an equal likelihood of being positive as it does of being negative. However, if a decay is indeed a source of TRV, then the triple product will have a preferred sign. Note that interactions between the final products may create a fake asymmetry, since the initial and final states are not interchanged.

## Design of the detector

### Scintillating material selection

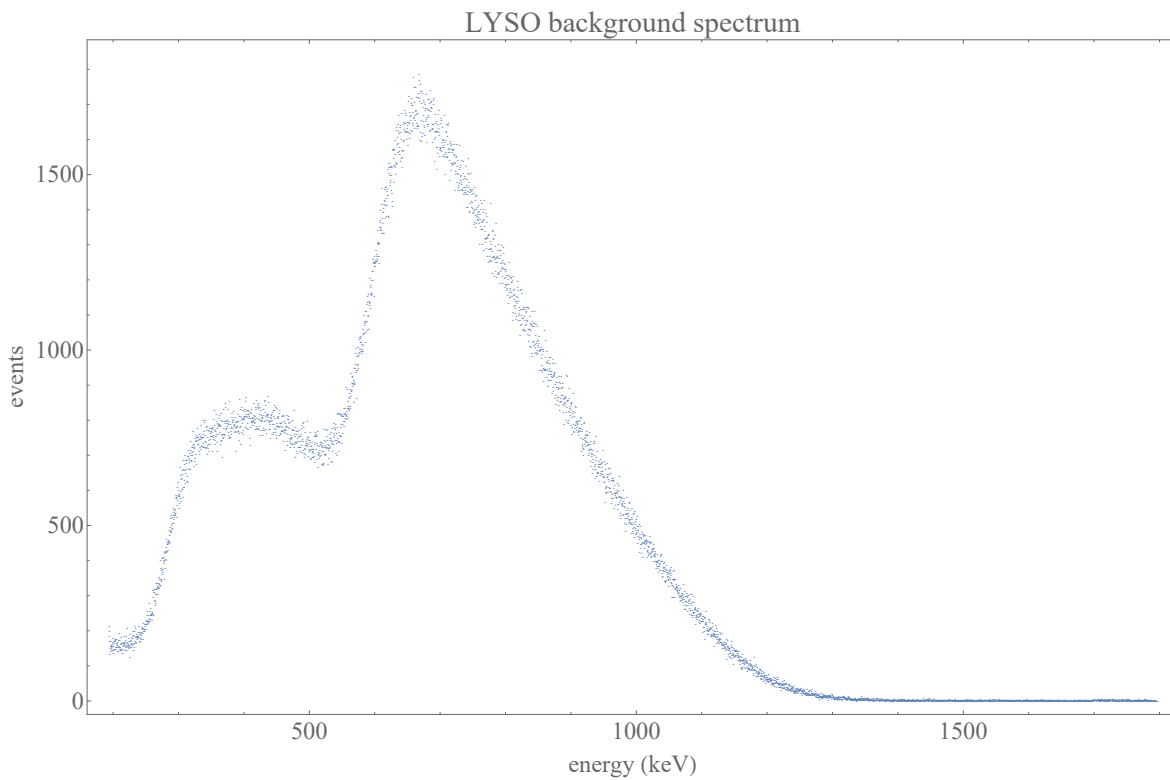
Before constructing the detectors, the scintillating material had to be selected. The three options (determined both by the price as well as the need to acquire two scintillators by September) were lutetium-yttrium-oxorthosilicate (LYSO), bismuth germanate (BGO), and sodium iodide doped with thallium (NaI(Tl)). Their properties are shown in Figure 2. LYSO and BGO are both significantly denser than sodium iodide (the former two have a density of about  $7 \text{ g/cm}^3$ , while sodium iodide's is  $3.6 \text{ g/cm}^3$ ), meaning that they will naturally be more efficient (i.e. they will detect a higher fraction of the photons that enter the scintillator and more often contain the total gamma energy). LYSO is faster and brighter than BGO; its wavelength of peak emission is also closer to the wavelength where the SensL SiPM is most efficient (420nm [4]). However, LYSO is slightly radioactive:  $^{176}\text{Lu}$  has a natural abundance of 2.6% and a half-life of 37 billion years [3]. Its  $\beta^-$  decay to  $^{176}\text{Hf}$  can emit any of eight gamma rays with energies between 800 and 1300keV. Since the decay of  $^{92}\text{Rb}$  radiates an 815keV gamma ray 3.2% of the time [3], the large number of gammas emitted by  $^{176}\text{Lu}$  in this energy range poses significant challenges. After examination of the background spectra of both crystals (presented in Figure 1) collected by a test board using a SensL 30035 SiPM model, BGO was chosen as the scintillating material which would be used in the gamma detectors.

### BGO crystal

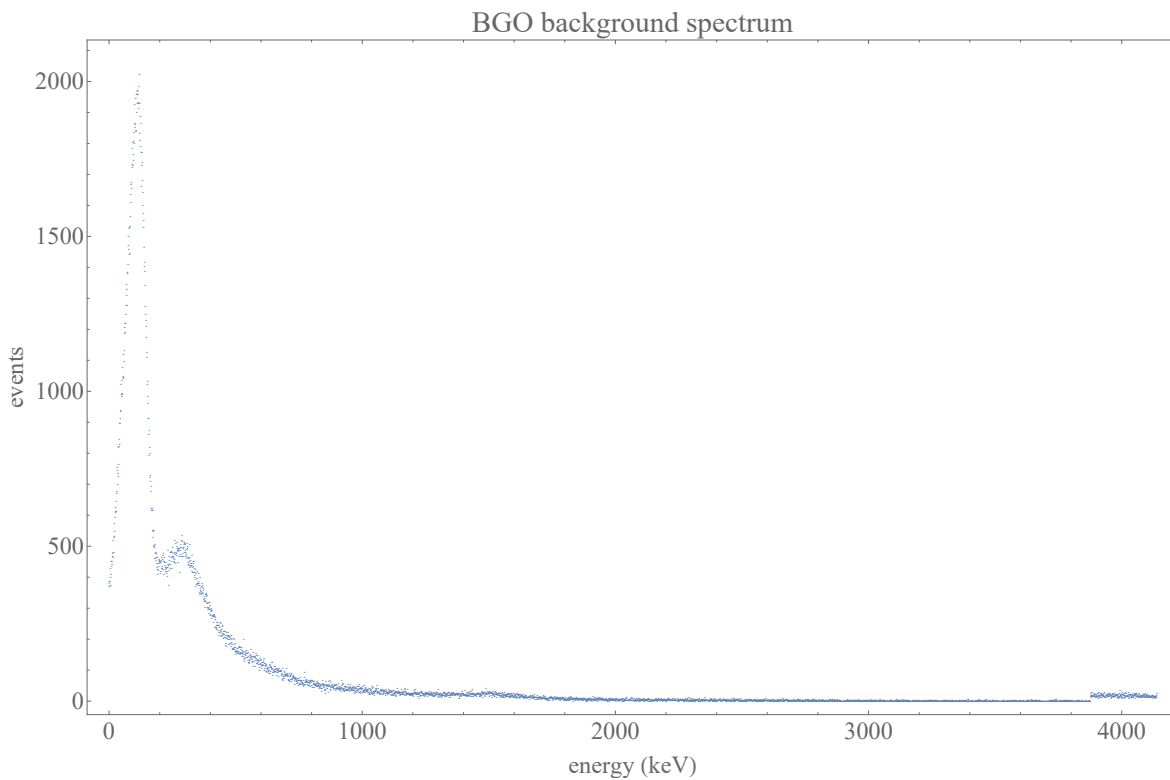
A scintillating BGO crystal coupled to an array of SiPMs comprises the core of each of the two detectors. As gamma rays enter the BGO, they produce scintillation light, which ideally should not escape the crystal. To that end, the crystal is surrounded by highly reflective material on all sides. The face closer to the center of the trap is entirely covered by a 3mm cylinder of Teflon (reflectivity coefficient of 0.99 at 440nm [6]). The lateral face of the cylinder is wrapped in a dielectric mirror film which reduces the likelihood of diffuse reflection as scintillating light reaches the edge of the BGO. The face farther away from the trap, which faces the silicon photomultiplier array, is painted with two layers of titanium dioxide. One layer of  $\text{TiO}_2$  has a reflectivity coefficient of 0.955 at 440nm [6], so two layers are likely as good a reflector as the Teflon on top of the cylinder. The titanium dioxide paint outlines a 25mm $\times$ 25mm square in the center of the bottom face of the BGO, through which the scintillating light passes to reach the SiPM array. The crystal and the electronics beneath it (discussed in the next section) are situated in a 3" optics tube capped in front of the 3mm Teflon by a 0.6mm light-tight aluminum cap. On top of this cap is another layer of Teflon, 0.635mm thick, designed to prevent beta particles from entering the scintillator. The extra Teflon accomplishes this at the cost of more brehmsstrahlung entering the detector.

### Silicon photomultiplier and readout

Between the BGO scintillator and the silicon photomultiplier array lies a 27mm by 27mm square of St. Gobain BG-634A silicone-based gel. This is due to the need to maximize the transmission of light from the BGO to the photomultipliers. This material (index of refraction 1.42) creates the best conditions for this since it transmits over 80% of incident light at angles up to  $45^\circ$  away from normal.



(a) Background spectrum of the LYSO scintillator. 1.97 million events in 20min.



(b) Background spectrum of the BGO scintillator. 390,000 events in 2hr 20min.

Figure 1: LYSO generated background events at roughly thirty-five times the rate of BGO, with the tail of the main peak extending to 1200keV. On the other hand, most events in the BGO were at low energies (which is why they form a pedestal at about 150keV).

	Specific Gravity	Wavelength of Max. Emission	Refractive Index	Decay Time ( $\mu$ s)	Abs. Light Yield in Photons/MeV	Relative Pulse Height Using Bialk. PM tube	References
<b>Alkali Halides</b>							
NaI(Tl)	3.67	415	1.85	0.23	38 000	1.00	
CsI(Tl)	4.51	540	1.80	0.68 (64%), 3.34 (36%)	65 000	0.49	78, 90, 91
CsI(Na)	4.51	420	1.84	0.46, 4.18	39 000	1.10	92
Li(Eu)	4.08	470	1.96	1.4	11 000	0.23	
<b>Other Slow Inorganics</b>							
BGO	7.13	480	2.15	0.30	8200	0.13	
CdWO <sub>4</sub>	7.90	470	2.3	1.1 (40%), 14.5 (60%)	15 000	0.4	98–100
ZnS(Ag) (polycrystalline)	4.09	450	2.36	0.2		1.3*	
CaF <sub>2</sub> (Eu)	3.19	435	1.47	0.9	24 000	0.5	
<b>Unactivated Fast Inorganics</b>							
BaF <sub>2</sub> (fast component)	4.89	220		0.0006	1400	na	107–109
BaF <sub>2</sub> (slow component)	4.89	310	1.56	0.63	9500	0.2	107–109
CsI (fast component)	4.51	305		0.002 (35%), 0.02 (65%)	2000	0.05	113–115
CsI (slow component)	4.51	450	1.80	multiple, up to several $\mu$ s	varies	varies	114, 115
CeF <sub>3</sub>	6.16	310, 340	1.68	0.005, 0.027	4400	0.04 to 0.05	76, 116, 117
<b>Cerium-Activated Fast Inorganics</b>							
GSO	6.71	440	1.85	0.056 (90%), 0.4 (10%)	9000	0.2	119–121
YAP	5.37	370	1.95	0.027	18 000	0.45	78, 125
YAG	4.56	550	1.82	0.088 (72%), 0.302 (28%)	17 000	0.5	78, 127
LSO	7.4	420	1.82	0.047	25 000	0.75	130, 131
LuAP	8.4	365	1.94	0.017	17 000	0.3	134, 136, 138
<b>Glass Scintillators</b>							
Ce activated Li glass <sup>b</sup>	2.64	400	1.59	0.05 to 0.1	3500	0.09	77, 145
Tb activated glass <sup>b</sup>	3.03	550	1.5	~3000 to 5000	~50 000	na	145
<b>For comparison, a typical organic (plastic) scintillator:</b>							
NE102A	1.03	423	1.58	0.002	10 000	0.25	

Figure 2: A table showing properties of various inorganic scintillators. Instead of containing values for LYSO, the table includes the closely related LSO. From [5].

For comparison, the absence of a coupling material (meaning that there is a thin layer of air between the BGO and the SiPMs) leads to 80% transmission of incident light only at angles below 10°.

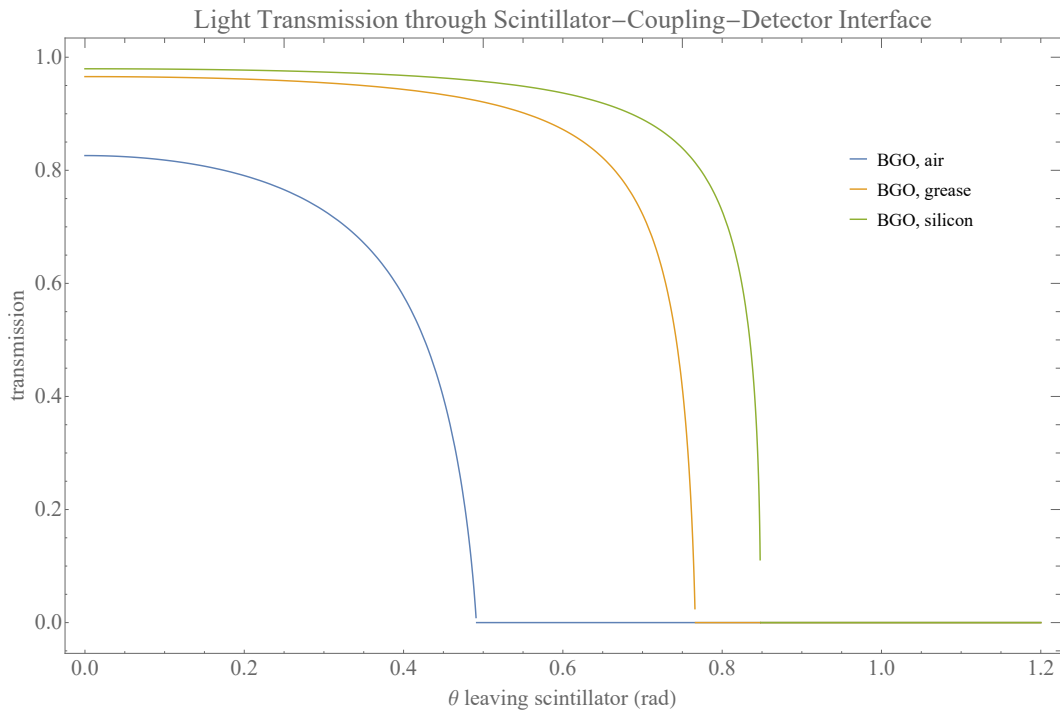


Figure 3: Effect of various coupling materials on the transmission of light from BGO to the SiPM array. The coupling material's curve used is labeled as silicon.

After the coupling silicone gel, the scintillation light enters one of four SensL ArrayJ-60035-4P PCB silicon photomultipliers. Each of these is a 2x2 array of smaller SiPM arrays, each of which contains 5,773 microcells [4]. Each array must be biased above its breakdown voltage (24.5V) for events to occur - during the run the SiPMs were biased to 30V i.e. 5.5V above the breakdown voltage.

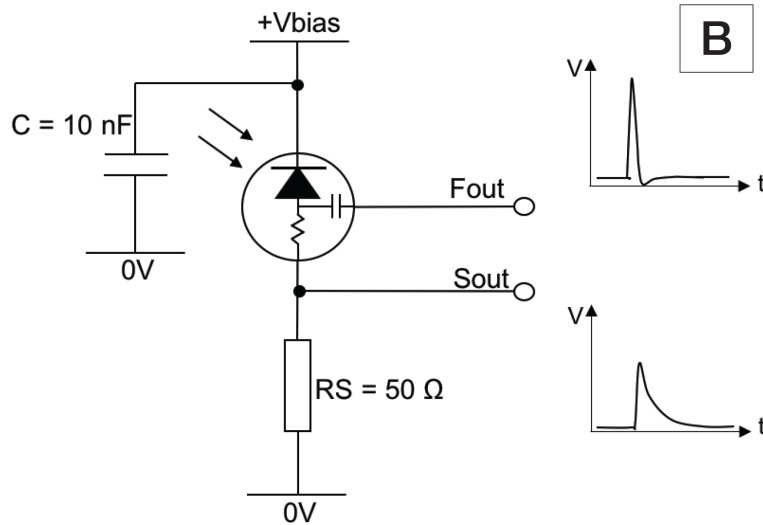


Figure 4: Biasing circuit used for each silicon photomultiplier. The fast output is only used in C-Series SiPMs and thus is not found in our photomultiplier. Additionally, the design used lacked a 10nF capacitor (the power supply provided a stable enough voltage). From [7].

Each 60035 SiPM has four outputs - one for each quarter of the device. Thus, the entire array has sixteen outputs which must be summed to obtain the total signal. This is accomplished by connecting four anodes to a common rail, each in the manner indicated in Figure 5. The lack of a coupling capacitor for each anode means that the timing of the circuit is decreased by a factor of 4; however, the slow response of the BGO (300ns characteristic time [5]) remains the limiting factor in determining the detector timing.

The sum of the four anodes is then connected to a pair of leads which snake out of the 3" optics tube in which the BGO and SiPM setup are located. The circuit board is backed by a layer of polyurethane to prevent light from leaking into the system. Light-tightness is further improved by wrapping the leads which carry the signals with copious amounts of black electrical tape. Finally, the leads connect to four coaxial cables, which carry the four signals to the analysis electronics. During data collection, the QDC gate time was set at 1600ns to collect the entire BGO signal, which has a rise time of approximately 320ns. If the beta trigger was selected instead of the gamma trigger in the acquisition system, the last 200ns of the gamma signal was cut off. This meant that the gamma spectrum acquired with the beta trigger was about 5% lower than the one obtained with the gamma trigger firing.

## Analysis electronics

The four coaxial cables which carry the anode voltages from SiPM readout circuit feed into a fan-in fan-out, which sums their signals. From here, the total signal is sent to two different locations. One cable is sent through a timing filter amplifier to a constant-fraction discriminator (CFD). The threshold of the CFD determines the height the signals must reach to be considered an event. Thus, its value plays a critical role in preventing noise from creating spurious events in the data acquisition system. The constant-fraction sends one signal to the time-to-digital converter (TDC) to determine the timing of the gamma signal relative to others. The CFD also sends a signal to the VME board, which generates a gate in which the signal should be found. The second output from the fan-out

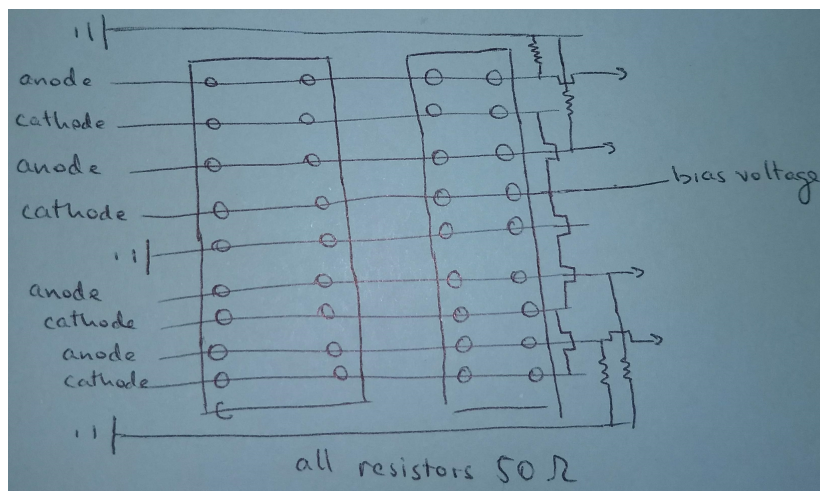


Figure 5: A sketch of the electronics connecting to the SiPMs. Bias voltage during beam time was 30V (5.5V above the breakdown voltage of 24.5V [4]). 50Ω resistors connect the anode rails to ground. The four anode wires each carry the combined signal of four anodes to the fan-in fan-out.

goes to the charge-to-digital converter (QDC), which records the total amount of charge entering it during the time specified by the gate from the VME. Thus, both outputs of the fan-out work together to determine whether an event occurred and to record the number of scintillating gamma rays that resulted from it.

## Data collection and analysis

During the experiment, it was discovered that only one detector (the one labeled #2) was working correctly; the #1 detector collected an overwhelming amount of low-energy events (see Figure 6). Thus, the analysis below focuses on the behavior of the #2 scintillator.

The first step in picking out true events from noise was identifying timing coincidences in the beta and gamma spectra. Random coincidences should not display any correlation between the timing of the events in the beta scintillator and the gamma detector. However, plotting events in the two detectors versus their relative timing shows a clear peak for both coincidences involving the second gamma detector (see Figure 7). Note that when selecting these events, a cut was made, throwing away all beta events with energies below the Compton edge of the 815keV  $^{92}\text{Rb}$  gamma. Most of the events below that energy (roughly 620keV) are gammas, so eliminating them reduced the number of random coincidences.

The next step was to plot the energies of the events in the timing peak. To calibrate the gamma QDC (i.e. relate each channel to an energy reading), a  $^{22}\text{Na}$  source was placed adjacent to the detector after the run. In its  $\beta^+$  decay,  $^{22}\text{Na}$  produces a 1274keV gamma ray. Furthermore, the positron emitted during the decay produces annihilation radiation and thus creates a peak at 511keV [3]. The spectrum is shown in Figure 8.

We can compare this calibration spectrum to the energy distribution of events in the timing peak mentioned above, shown in Figure 9.

There are four notable features in this spectrum: the pedestal at around channel 300, the 511keV peak at about channel 1000, a small shoulder on the tail of that peak near channel 1300, and a rise above channel 3500 (likely cosmic ray events). The 511keV peak is likely caused by brehmsstrahlung and  $e^-e^+$  annihilations from high-energy betas near the beta detector. The channel 300 threshold mainly consists of background events that happened to fall within the timing peak. The feature of interest is the peak at channel 1300. Calibration of the BGO based on the  $^{22}\text{Na}$  spectrum gives the following energy calibration:

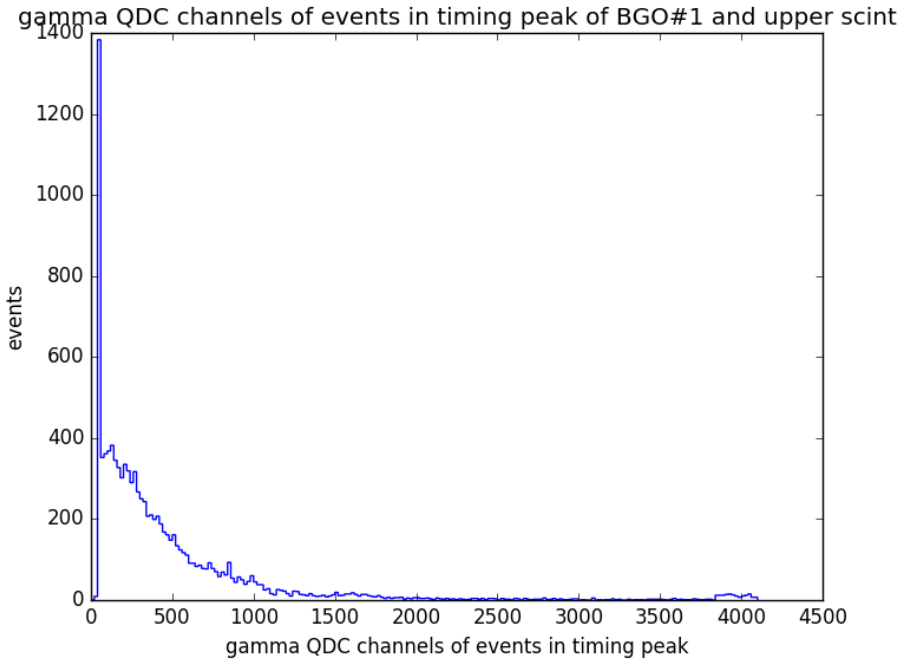


Figure 6: Detector #1 appeared to have a source of low-energy events (as evidenced by the peak at around channel 40).

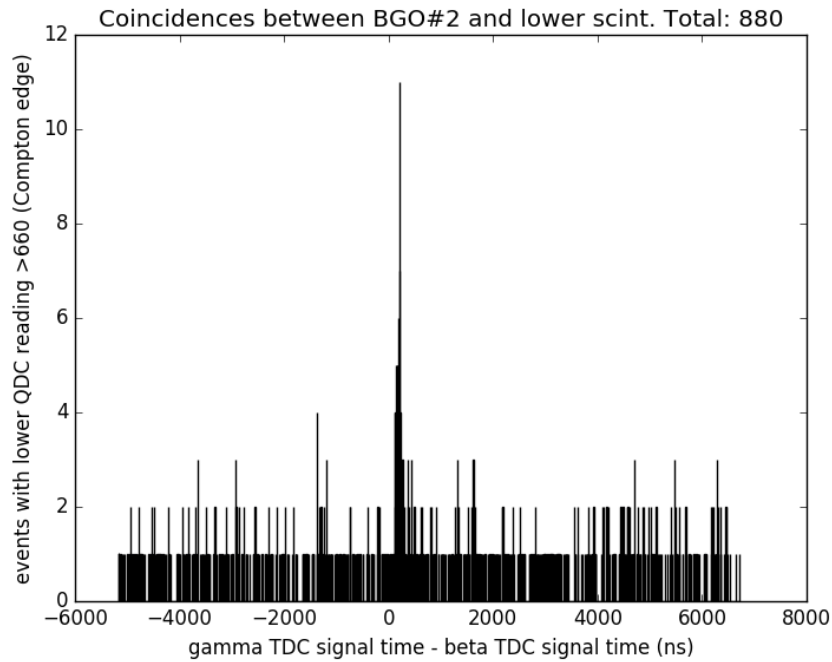


Figure 7: The relative timings of events in the second gamma detector and the bottom beta scintillator. A clear peak is visible at about 200ns. In the corresponding plot of timing between the second gamma detector and the top beta scintillator, the peak is at about 300ns (the difference is likely due to cabling).

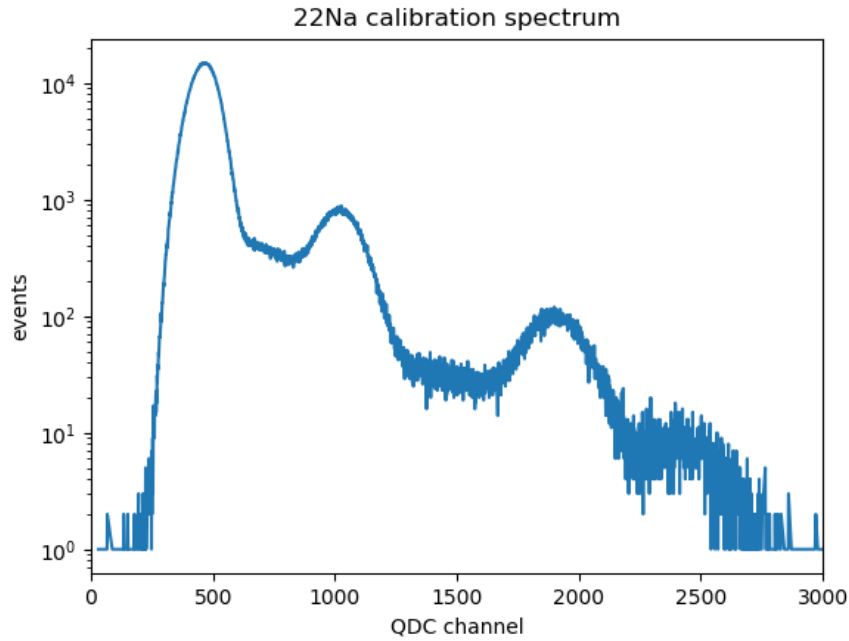


Figure 8: A log plot of the calibration spectrum of the BGO. The 511keV and 1274keV peaks, as well as their sum peak, are visible. The peak just below channel 500 is due to low-energy noise.

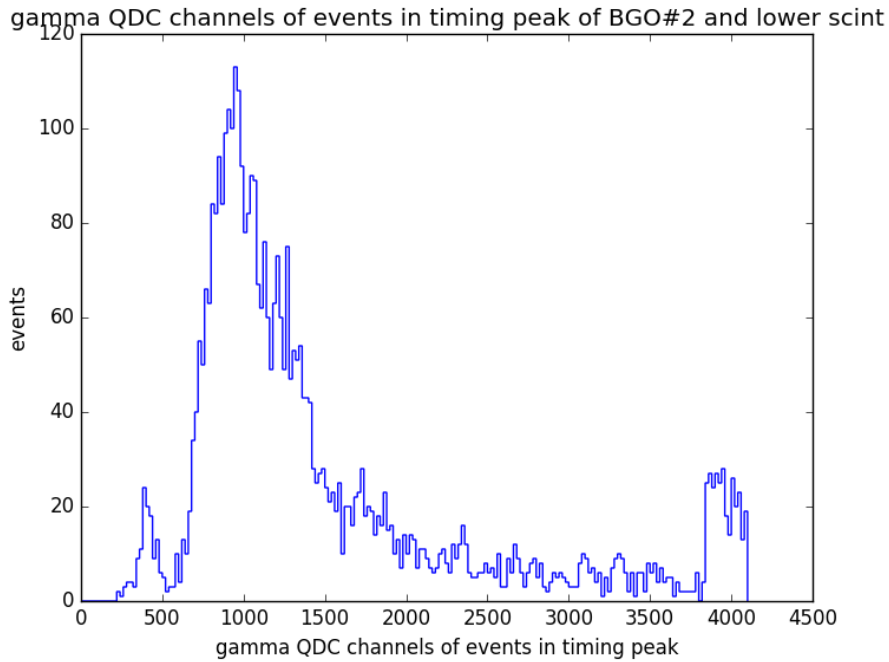


Figure 9: The energy spectrum of events in the timing peak. The 511keV peak (from brehmsstrahlung in the Teflon) has a shoulder at about channel 1300. This is the 815keV gamma from the  $^{92}\text{Rb}$  decay.

$$E_\gamma \text{ (keV)} = 0.8573 \frac{\text{keV}}{\text{channel}} \times \text{channel} - 363 \text{ keV}$$

Using this as a calibration places 815keV at roughly channel 1370. Taking into consideration that the peak in the spectrum will be shifted toward a lower channel, since it lies on the tail of the 511keV peak, it is reasonable to conclude that it is indeed the 815keV gamma from  $^{92}\text{Rb}$  decay. The fact that the BGO is sensitive enough to show a recognizable peak from a gamma ray that is produced only 3.2% of the time bodes well for future runs, where the decay of  $^{38m}\text{K}$  will be examined for time reversal violation.

## Conclusion

This summer's work involved the design, construction, and calibration of two gamma ray detectors, which were mounted on the TRIUMF Neutral Atom Trap. The demonstration that one of the detectors was able, after some filtering, to pick out a gamma ray from a 3% branch of the  $^{92}\text{Rb}$  decay indicates that the design is fundamentally sound. This provides a guide toward improving the detectors - perhaps by replacing the BGO with a more expensive scintillating material with better energy resolution e.g. germanium or a newer inorganic scintillator like GAGG - for future runs involving  $^{38m}\text{K}$  and/or  $^{37}\text{K}$ .

## Acknowledgements

First and foremost, I would like to thank my mentor, Dr. John Behr. The countless hours he spent in the lab with me were invaluable. Thanks also to the other members of the TRINAT group (Dr. Alexandre Gorelov, Dr. Melissa Anholm, James McNeil, and Daniel Schultz), as well as my co-mentor, Dr. Petr Vogel.

## References

- [1] Andrei Sakharov. Violation of cp invariance, c asymmetry, and baryon asymmetry of the universe. *ZhETF Pisma*, 5:32–35, 1967.
- [2] John Behr. TRIUMF EEC Progress Report Detailed Statement S1603 - TRV in  $\beta\nu\gamma$  decay. 2018.
- [3] Brookhaven National Laboratory. Chart of Nuclides.
- [4] SENSL. *ArrayJ - High Fill-Factor Arrays of J-Series SiPM Sensors*, March 2018.
- [5] Glenn F. Knoll. *Radiation Detection and Measurement*. John Wiley and Sons, 4th edition, 2010.
- [6] Martin Janecek. Reflectivity Spectra for Commonly Used Reflectors. Technical report, US Department of Energy, 2012.
- [7] SENSL. *Biasing and Readout of SensL SiPM Sensors*, March 2018.